

Structural transition and uranium valence change in UTe_2 at high pressure revealed by x-ray diffraction and spectroscopy

Yuhang Deng^{1†}, Eric Lee-Wong^{1†}, Camilla M. Moir¹, Ravhi S. Kumar², Nathan Swedan¹, Changyong Park³, Dmitry Yu Popov³, Yuming Xiao³, Paul Chow³, Ryan E. Baumbach^{4,5}, Russell J. Hemley⁶, M. Brian Maple^{1*}

¹Department of Physics, University of California, San Diego, CA 92093, USA

²Department of Physics, University of Illinois Chicago, Chicago, IL 60607, USA

³High Pressure Collaborative Access Team, X-ray Science Division, Argonne National Laboratory, Argonne, IL 60439, USA

⁴National High Magnetic Field Laboratory, Florida State University, Tallahassee, FL 32306, USA

⁵Department of Physics, Florida State University, Tallahassee, FL 32306, USA

⁶Departments of Physics, Chemistry, and Earth and Environmental Sciences, University of Illinois Chicago, Chicago, IL 60607, USA

†These authors contributed equally to the work.

*Corresponding author: M. Brian Maple. Email: mbmaple@ucsd.edu

Abstract

High pressure x-ray diffraction up to 30 GPa in conjunction with resonant emission x-ray spectroscopy and partial fluorescence yield x-ray absorption spectroscopy up to 52 GPa were used to study how the structural and electronic properties of UTe_2 evolve with pressure at room temperature. An orthorhombic to tetragonal phase transition was observed to occur between 5 and 7 GPa, with a large volume collapse of nearly 11% and a nearest U-U distance increase by about 4%. This lower to higher symmetry transition suggests less $5f$ electron participation in bonding when the weakly correlated superconducting phase in the tetragonal structure of UTe_2 appears. Beyond 7 GPa, no new structural transitions were found up to 30 GPa. The resonant x-ray emission spectra clearly demonstrate an intermediate valence of U, nearly +3.74 at 1.8 GPa and room temperature, and reveal that the U valence shifts towards 4+, passes through a peak at 2.8 GPa, and then decreases towards 3+ and settles to a nearly constant value above 15 GPa. These experiments reveal that some fundamental structural and valence changes occur in UTe_2 at relatively low pressures, which could be responsible for the interplay between unconventional superconductivity, magnetic ordering, and weakly correlated superconductivity that is manifested in the temperature-pressure phase diagram of UTe_2 .

Introduction

The heavy fermion f -electron superconductor UTe_2 has attracted a great deal of attention, driven by an interest in developing a fundamental understanding of its extraordinary unconventional superconducting properties and the possibility that it exhibits spin-triplet superconductivity with potential applications in quantum computation [1, 2]. The compound UTe_2 has an enormous re-entrant upper critical field $H_{c2}(T)$ of the order of 40 T, considering its low superconducting critical temperature T_c of only 2 K. In addition, there is a pocket of high magnetic field superconductivity (so-called Lazarus phase) which occurs at magnetic fields B between 40 T and 60 T and at angles θ between 23° and 45° , where θ is measured with respect to the b axis in the b - c plane of the UTe_2 body-centered orthorhombic unit cell [3, 4].

Our approach to study the electronic properties of UTe_2 uses pressure (P) to tune electronic interactions in UTe_2 . Pressure (P) is a clean and powerful parameter for tuning electronic interactions in quantum materials, often resulting in dramatic changes in physical properties in the vicinity of a critical pressure P_c at which a second order phase transition has been suppressed to 0 K, referred to as a quantum critical point (QCP). Remarkably, unconventional forms of superconductivity and exotic magnetic phases are often found in the vicinity of the QCP. We applied two different spectroscopic techniques, U L_3 edge Partial Fluorescence Yield X-ray Absorption Spectroscopy (PFY-XAS) and Resonant X-ray Emission Spectroscopy (RXES), to explore the U valence change and the degree of $5f$ electrons delocalization in UTe_2 under high pressure. The U L_3 edge was chosen because of the better energy resolution from the longer $3d$ core-hole lifetime (~ 4 eV) compared to the $2p$ core-hole lifetime (~ 8 eV) [5]. The $L_{\alpha 1}$ emission from the $3d$ to $2p$ transition was found to split due to different screening effects on the $2p$ core hole by the $5f$ -electron in different configurations [6, 7], pointing unambiguously to the multiconfigurational features of U in UTe_2 . X-ray Diffraction (XRD) measurements under high P were also used to determine the P -dependence of the lattice parameters a , b , and c , and volume of the body-centered orthorhombic unit cell of UTe_2 , and search for possible crystallographic phase transitions. Measurements were taken at room temperature (RT) up to 30 GPa for XRD and up to 52 GPa for PFY-XAS and RXES.

From XRD data, we observed a structural phase transition from the body-centered orthorhombic structure (space group $Immm$) to the body-centered tetragonal structure (space group $I4/mmm$) in the range of 5 – 7 GPa, confirming the results in Refs. [8, 9] at ~ 5 GPa and ~ 4 GPa respectively. A nonmonotonic change in the U L_3 white-line position was seen in the PFY-XAS spectra, which indicates a pressure-induced change in the U valence or a change in the degree of localization of the $5f$ electrons. From RXES measurements, we found evidence for an initial increase in the U valence toward $4+$ up to 2.8 GPa, in partial agreement with the XANES measurements in Ref. [10] and the XANES and X-ray magnetic circular dichroism (XMCD) measurements in Ref. [11]. Strikingly, with increasing pressure beyond 2.8 GPa, the U valence drops toward $3+$ until ~ 15 GPa where it remains stable up to 52 GPa. The unusual U valence change and the appearance of the high-pressure tetragonal phase harboring a new superconducting state [9] may be related and warrants further investigation.

Experimental Methods

UTe_2 single crystals were grown by chemical vapor transport and then powdered for measurements. Two batches of samples (S1 and S2) were measured in this work. Batch S1 was synthesized using the following procedure: uranium and tellurium in a 2:3 atomic ratio were sealed in a quartz tube with 3 mg/cm^3 of iodine and kept at a temperature gradient of 1060°C at the hot end and 1000°C at the cold end for 2 weeks. Batch S2 was grown following the method described in Ref. [12]. Two high-pressure XRD runs on S1 and S2 were carried out at RT in beamline 16-BMD of HPCAT, the Advanced Photon Source (APS) in Debye-Scherrer geometry. Uranium L_3 edge RXES and PFY-XAS data at RT under various pressures were collected using samples from batch S2 at the HPCAT 16-IDB beamline. More details are in Supplementary Materials [13].

Results and Discussion

High-pressure XRD

Figure 1 shows waterfall plots of the UTe_2 (S1 and S2) XRD spectra under high pressure up to 30 GPa and 20 GPa, respectively. At near ambient pressure, UTe_2 spectra was identified with an orthorhombic structure and space group $Immm$ [14] with no impurities. Obvious changes in the diffraction patterns, seen in Figure 1(b), between 5 and 7 GPa, indicate that a structural phase transition has occurred. The transition is complete at ~ 8 GPa, which agrees with results of Refs. [8, 9], with no further phase transitions observed up to 30

GPa. Small discrepancies in the transition pressure could be explained by our choice of different pressure transmitting media.

The reduced number of peaks in the XRD spectra of the high-pressure phase indicates an increased symmetry, which was identified as a body-centered tetragonal structure (space group $I4/mmm$) [15, 8, 9]. Following the analyses in Refs. [15, 8, and 9], the lattice parameters (a , b , c), and unit cell volume (V) of UTe_2 under pressure were calculated via Rietveld refinement of XRD peaks using the open-source software GSAS-II [16], shown in Figure 2. The atomic positions of U and Te atoms in the unit cell of the orthorhombic/tetragonal phase were also refined and to find the pressure dependence of the nearest uranium to uranium distance, d_{U-U} , in Figure 3. The initial unit cell volume (V_0) was refined from ambient pressure XRD spectra taken at RT from the same batch used in subsequent high pressure XRD measurements.

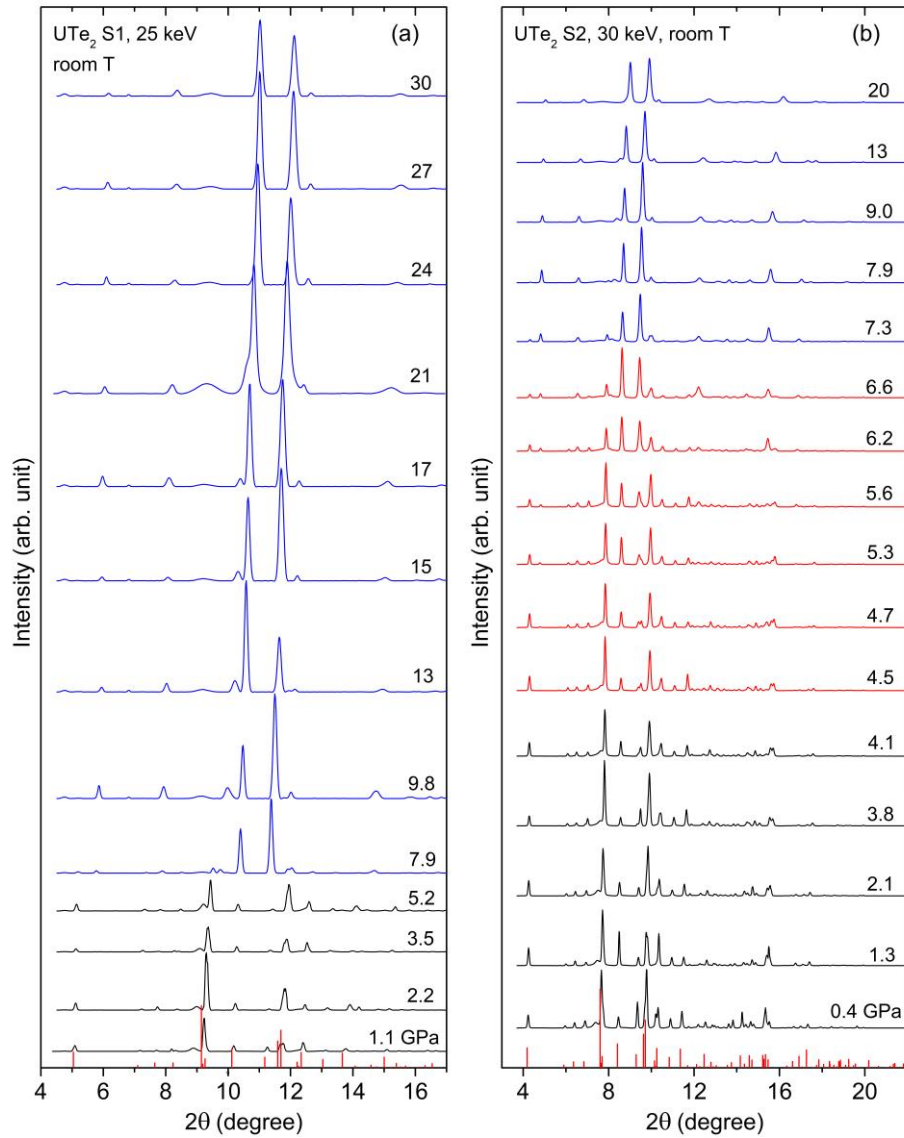


Figure 1. XRD spectra of UTe_2 measured at various pressures between 0.4 and 30 GPa. (a) XRD patterns of UTe_2 from batch S1; (b) XRD spectra of UTe_2 from batch S2, which show a structural phase transition in progress between 5 GPa to 7 GPa. The color scheme used to delineate the XRD spectra: Black - low- P

phase, blue – high- P phase, red – mixed low- P and high- P phases. Red vertical lines at the bottom of the figures indicate standard UTe_2 diffraction peaks based on Ref. [14].

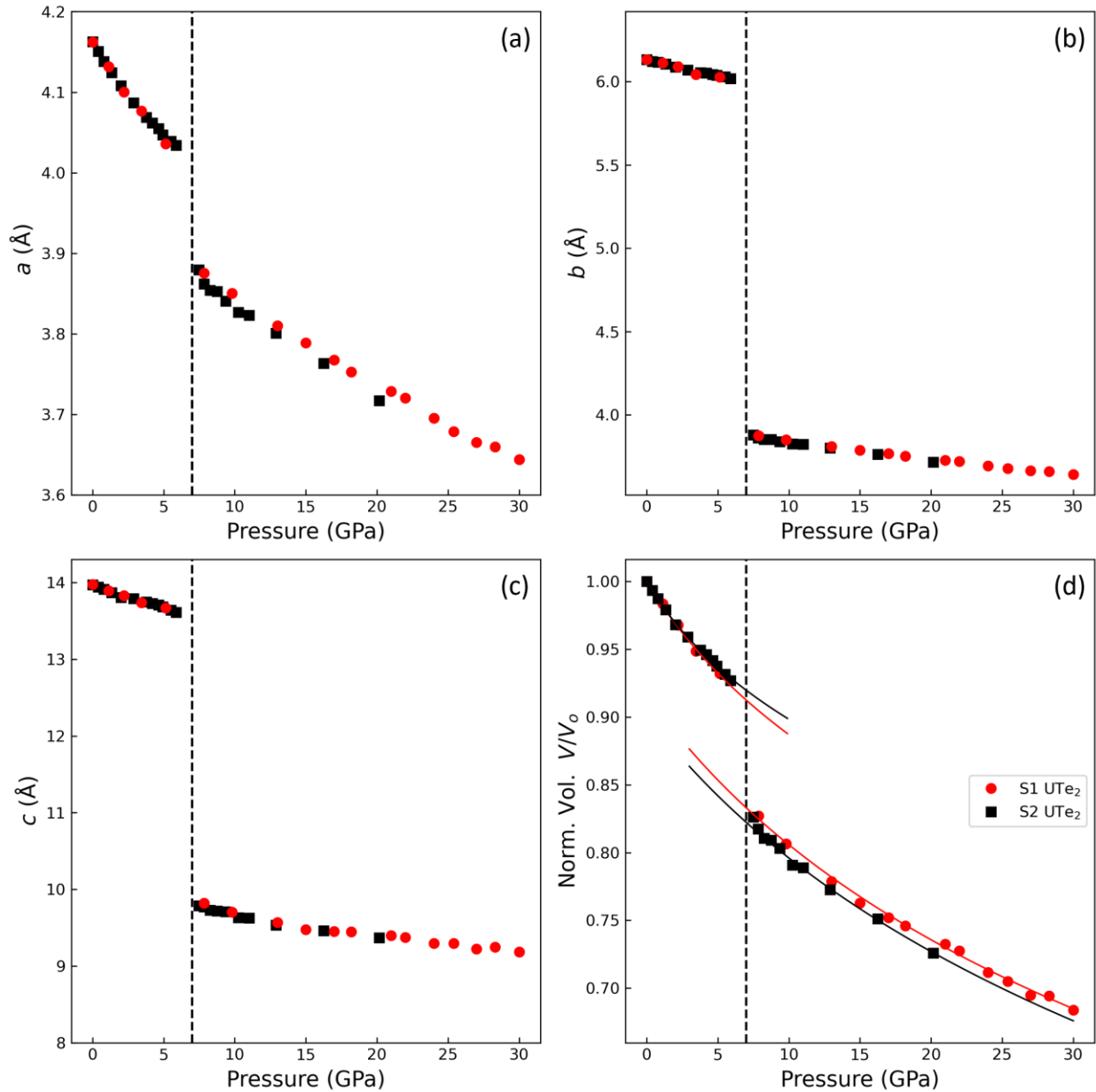


Figure 2. Lattice parameters for two samples of UTe_2 vs. pressure. (a - c): Lattice parameters a , b , and c . The current figure omits data points from the mixed phase for simplicity. (d): Normalized unit cell volume (V/V_0) vs. increasing pressure with respective 3rd order Birch-Murnaghan equation of state fits for both phases. The tetragonal phase V was multiplied by 2 and normalized to the $Immm$ V_0 to conserve the number of atoms across the structural phase transition.

Both samples of UTe_2 exhibit a relative volume decrease of $\Delta V/V_0 \sim 11\%$ at the phase transition (Figure 2(d)). The b axis of the low-pressure orthorhombic lattice has the largest compression of $\sim 33\%$ at the phase

transition, followed by $\sim 27\%$ for the c axis and $\sim 3\%$ for the a axis. The bulk modulus (K_0) and differential bulk modulus (dK_0/dP) were calculated by fitting a 3rd order Birch-Murnaghan equation of state [8] to the V vs. P data,

$$P(V) = \frac{3}{2}K_0 \left[\left(\frac{V_0}{V} \right)^{\frac{7}{3}} - \left(\frac{V_0}{V} \right)^{\frac{5}{3}} \right] \times \left\{ 1 + \frac{3}{4} \left(\frac{dK_0}{dP} - 4 \right) \left[\left(\frac{V_0}{V} \right)^{\frac{2}{3}} - 1 \right] \right\} \quad (1)$$

In Table 1, we list the fitting parameters of the 3rd order Birch-Murnaghan equation of state for our data shown in Figure 2(d).

Table 1. V_0 , K_0 , and dK_0/dP of UTe_2 in the orthorhombic and tetragonal phases at RT.

	Orthorhombic ($Immm$)			Tetragonal ($I4/mmm$)		
	V_0 (\AA^3)	K_0 (GPa)	dK_0/dP	V_0 (\AA^3)	K_0 (GPa)	dK_0/dP
UTe_2 S1	356.73	60 ± 5	6 ± 3	163.31	62 ± 13	3.6 ± 0.7
UTe_2 S2	356.63	57 ± 4	6.2 ± 2	160.31	67 ± 2	3.3 ± 0.4

The value of K_0 (avg. ~ 59 GPa) for the orthorhombic phase is comparable to that in Refs. [8] (~ 44 GPa) and [9] (~ 59 GPa). The high-pressure tetragonal UTe_2 phase has a stiffer bulk modulus of ~ 65 GPa, which is smaller than the value (~ 74 GPa) obtained in [8]. The bulk modulus of the orthorhombic phase is small, comparable to tellurium (65 GPa), suggesting UTe_2 is a very soft material whose physical properties are more responsive to changes in pressure. Interestingly, tellurium also undergoes a hexagonal to monoclinic structural transition at about 4 GPa, which is similar to the onset pressure for the structural phase transition for UTe_2 [17].

The change in d_{U-U} with pressure was also calculated (shown in Figure 3) for the two structures. Notably, d_{U-U} increased at the structural phase transition, from ~ 3.7 \AA to ~ 3.9 \AA , comparable to the values reported in Refs. [9] and [8]. Even at 30 GPa, the d_{U-U} is still above the Hill limit of uranium compounds (3.4 - 3.6 \AA).

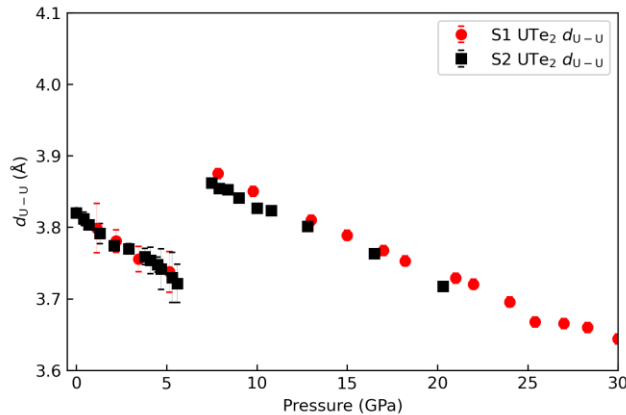


Figure 3. The change in d_{U-U} in UTe_2 with pressure. For both samples, d_{U-U} increases at the structural phase transition from $Immm$ to $I4/mmm$ and steadily decreases with increasing pressure, where d_{U-U} in the high-pressure tetragonal phase at ~ 20 GPa equals the value in the lower pressure orthorhombic phase at 6 GPa. The vertical bars represent the d_{U-U} measurement uncertainty. See Ref. [13] for details.

Using the CALYPSO software package and Vienna ab initio simulation package (VASP), Hu *et al.* predicted that the $Immm$ to $I4/mmm$ structural transition would occur at 4 GPa accompanied by a $\sim 12\%$ volume collapse at the transition, when implementing the Perdew-Burke-Ernzerhof (PBE) + Hubbard U method with $U = 1$ or 2 eV [15]. This value is quite comparable to our experimental results of $\sim 11\%$ decrease in volume. The denser high pressure $I4/mmm$ phase is achieved through a transition from a U-Te eight-coordinated distorted square antiprism [8] to a ten-coordinated “bicapped cube”, in which lone pair electrons of Te participate more in forming covalent bonding with U atoms, according to the calculation of the projected two-dimensional electron localization functions [15].

Crystallographic and electronic structures are intimately interrelated, which underlines the importance of studying the pressure induced structural phase transition in UTe_2 , since it can provide insights into how $5f$ -electrons are involved in the bonding. When more $5f$ -electrons participate in bonding in actinides it is typical to observe lower crystallographic symmetry [18, 19]. With respect to the behavior of UTe_2 under pressure, the d_{U-U} in UTe_2 (~ 3.8 Å) at ambient pressure is larger than the Hill limit (~ 3.5 Å), a “rule-of-thumb” parameter representing the boundary between localization and delocalization of $5f$ -electrons for U compounds. Thus, we should expect magnetic order in UTe_2 instead of the superconductivity [20] observed in UTe_2 at ambient pressure. Strangely, the increase in d_{U-U} at ~ 5 GPa indicates the $5f$ -electrons of UTe_2 become more localized under pressure, which is consistent with the transition from the lower symmetry orthorhombic phase to the higher symmetry tetragonal phase, if the correspondence between $5f$ -localization and higher crystal structure symmetry is applicable to UTe_2 . The scenario of increased localization of $5f$ -electrons in UTe_2 under pressure is supported by measurements of the electrical resistivity as a function of temperature reported in Ref. [9]. The measurements reveal the occurrence of superconductivity above 6 GPa with an upper critical field lower than the Pauli limit and Fermi liquid behavior in the normal state electrical resistivity $\rho(T)$ with a small coefficient of the T^2 term, indicating that the electronic state of tetragonal UTe_2 is weakly correlated [9].

Huston *et al.* [8] pointed out that in other uranium chalcogenides such as USe and UTe which have a ferromagnetic ground state and a d_{U-U} that exceeds the Hill limit, pressure also drives a transition from lower to higher structural symmetry [21, 8]. It is interesting to note, regardless of whether the ground state is superconducting as in UTe_2 , or ferromagnetic as in USe and UTe, uranium chalcogenides seem inclined to transform into a higher symmetry phase at high pressure. In the first-principles study of UTe_2 by Hu *et al.*, it was shown that covalent bonding between lone pair electrons of Te and U atoms forms in the high-pressure tetragonal phase [15]. Perhaps this covalent bonding localizes $5f$ -electrons, thus inducing the higher symmetry tetragonal phase and increasing the bulk modulus appreciably since a three-dimensional network of covalent bonds (e.g., diamond and quartz) is usually quite rigid (although lattice stiffening is common in many kinds of pressure induced phase changes) [22].

High-pressure PFY-XAS

The electronic configuration of U in UTe_2 at ambient or high pressures has been studied using a variety of x-ray spectroscopy techniques [10, 11, 23]. Here we explore the PFY-XAS of the U L_3 absorption from $2p_{3/2}$ to an unoccupied $6d$ orbital and the RXES of the U $L_{\alpha 1}$ emission from $3d_{5/2}$ to $2p_{3/2}$ to study the electronic state of UTe_2 . PFY-XAS measurements were taken by exciting the U L_3 absorption edge with incident energy between 17.140 - 17.210 keV, while detecting emission at the U $L_{\alpha 1} = 13.614$ keV line. Measurements were performed at RT at various pressures in DACs. As can be seen in Figure 4, our PFY-XAS spectra for UTe_2 show the white-line (main peak) from the $3d_{5/2}$ to $2p_{3/2}$ transition, a step-function like background associated with the excitation into the continuum above the $6d$ states, and a small pre-edge shoulder at 6-7 eV below the white-line. The shoulder can be attributed to a pre-edge quadrupole transition from $2p_{3/2}$ to $5f$ [24], which is usually smaller compared to the dipole allowed white-line. A similar feature on the left side of the white-line was also found in U^{4+} , U^{5+} , and U^{6+} compounds, with a separation of 5-7

eV [24, 25]. PFY-XAS spectra was normalized to the post-edge step above 17.170 keV due to the excitation into the continuum using the open-sourced Larch XAS analysis software [26], while additional post white-line flattening was applied to the data at $P = 1.8$ GPa due to synchrotron beam current instability that occurred during measurement (subsequent measurements did not have this issue). Spectra were fitted with a combination of an arctangent step function for data above 17.170 keV and a Gaussian function for the white-line, using the method outlined by Ref. [10]. The model was adjusted by varying all parameters with initial guesses for the step function width set to the uranium L_3 core-hole lifetime (~ 3.9 eV) and the step function position set by the first derivative of the interpolated PFY-XAS data curve. A detailed description and a figure showing all deconvoluted PFY-XAS spectra are presented in Supplementary Materials [13].

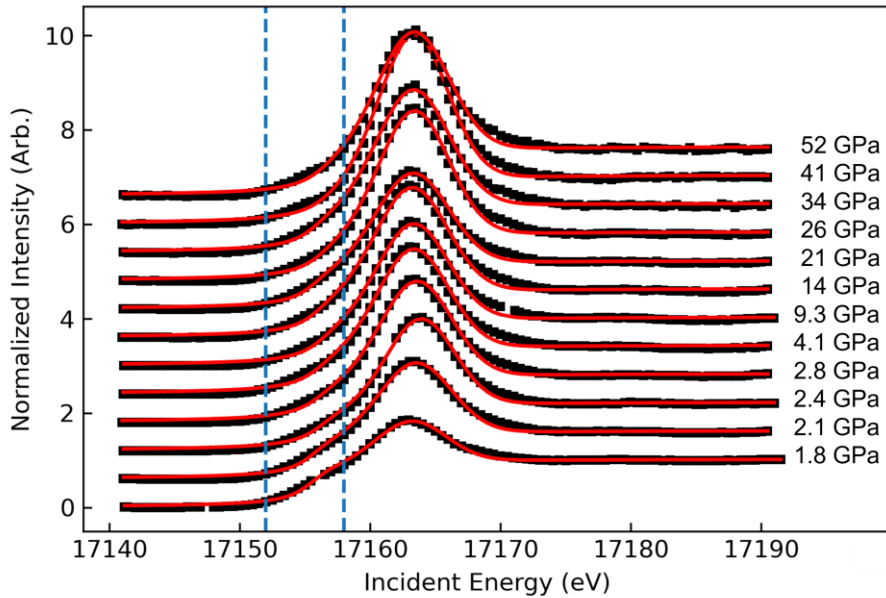


Figure 4. PFY-XAS spectra of UTe_2 at different pressures. Curves are offset vertically for clarity. The emission intensity is normalized to the incident intensity. The two blue dashed lines enclose the region where the pre-edge quadrupole resonance occurs. The red curves are fits to the data which are represented by solid black squares (see Supplementary Materials [13] for more discussion).

Figure 5 shows the change in the white-line peak position under pressure, which was found by plotting the E_i of the peak maximum (see [13]). The white-line position blueshifts by ~ 0.7 eV up to 2.4 GPa. However, subsequent increases in pressure results in a redshift white-line up to 4.1 GPa, after which there is little change in peak position up to 52 GPa. In previous studies of uranium intermetallics, changes in the U L_3 edge white-line position were attributed to a change in U valence (or $5f$ -electron count) [10] or a change in the degree of delocalization of the $5f$ -electrons [7]. Although there are contradictory conclusions on the $5f$ -electron count of UTe_2 (closer to 3 [27, 11] vs closer to 2 [10]) at ambient pressure, UTe_2 is believed to have an intermediate valence. Thomas *et al.* reported a small increase in U valence towards $4+$ above 1.25 GPa [10] in UTe_2 under pressure. Using U $M_{4,5}$ edge XANES, Wilhelm *et al.* [11] observed an initial increase in valence towards $4+$ with pressure up to ~ 2 GPa, followed by a decrease in valence back to $3+$ with pressure. The white-line blueshift below 2.4 GPa can be ascribed to a pressure-induced delocalization of $5f$ -electrons, or a transfer of spectral weight from $5f^3$ to $5f^2$ configuration, or a combination of both. Considering that the d_{U-U} is larger than the Hill limit, delocalization can occur through the hybridization between the conduction band and $5f$ orbitals. Between 2.4 and 4.1 GPa, the observed redshift of the L_3 white-line indicates a reverse trend: $5f$ -electrons become more localized or there is an increase in the

occupancy of the $5f^3$ configuration. The stable white-line position between 4.1 and 52 GPa reveals a $5f$ configuration with a stable degree of localization or a stable $5f$ configuration. The multiple origins of the white-line shift and the limited resolution of PFY-XAS data prevented an estimation of the $5f$ occupancy using standard first x-ray sum rules [28], so an estimation of the $5f$ occupancy was determined from deconvoluting RXES data instead, as described below.

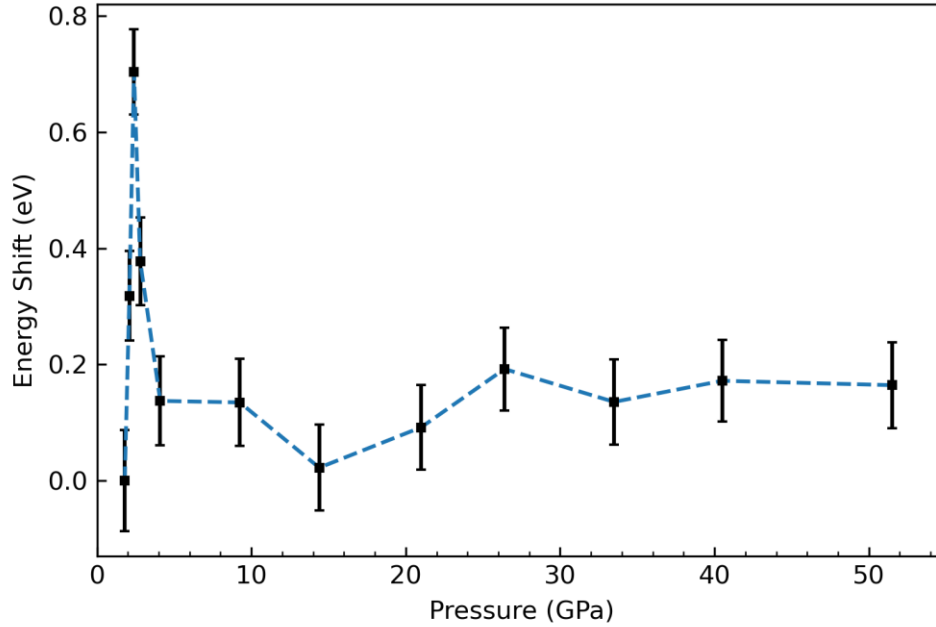


Figure 5. Change in UTe_2 S1 U L_3 edge white-line position for UTe_2 with pressure relative to its position at 1.8 GPa. The vertical bars indicate the fitting error determined by estimated standard deviation [13].

High pressure RXES

Representative RXES spectra of normalized $L_{\alpha 1}$ emission of UTe_2 at 2.1 GPa are shown in Figure 6 as a function of incident x-ray energy (E_i) and transferred energy $E_t \equiv E_i - E_e$ where E_e is the emission energy. Even before deconvoluting configuration peaks there is a distinguishable doublet in the spectra at E_t below the white-line. Peak positions stay nearly constant with E_t when E_i is lower than a threshold $E_T = 17.170$ keV above which the non-resonant x-ray emission becomes dominant. This is characteristic of the resonant emission from $3d_{5/2}$ to $2p_{3/2}$ [5]. When E_i is higher than E_T , the excitation into the continuum overwhelms the excitation into the $6d$ states, and the emission spectra as a function of E_t shift linearly with E_i [5, 6], as indicated by curves with $E_i > E_T$ in Figure 6. The multiple peaks in the RXES emission spectra indicate multiconfigurational $5f$ states and agrees with the PFY-XAS results. This suggests UTe_2 falls into a similar grouping of intermediate valence materials like SmB_6 , $YbAl_3$ [29], and UPd_2Al_3 [30].

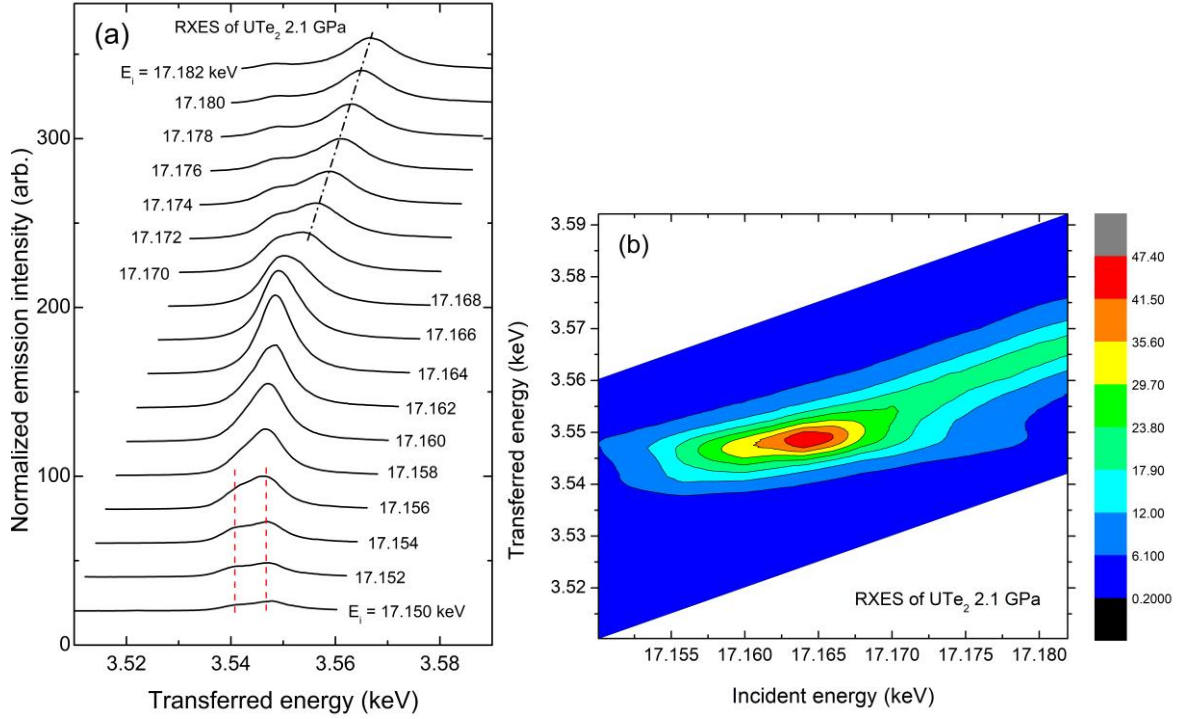


Figure 6. RXES of UTe_2 S1 at 2.1 GPa and RT. The red dashed lines indicate the two $5f$ configurations and the black dash-dotted line indicate the shift in the non-resonant emission. The colors in the vertical scale bar of (b) show the normalized emission intensity. When $E_i \geq 17.170$ keV, a clear linear correlation can be seen between E_t at the emission maximum and E_i , indicating emission is from non-resonant excitation to the continuum.

The $5f$ configuration weights ($5f^3$, $5f^2$) were calculated using the methodology in Ref. [6] for UCd_{11} and PuSb_2 . Since the total number of unoccupied $6d$ states is almost fixed, the relative excitation amplitude should be proportional to the occupancy in each $5f$ configuration [6]. The $5f$ -electron occupancy can then be calculated from the weighted sum of the integrated multiconfiguration peaks that are deconvoluted from the RXES spectra. Fortunately, unlike some other U intermetallics (e.g., UCd_{11} [6], URu_2Si_2 [25]), our RXES data at energy below E_T clearly exhibit separate f^3 and f^2 peaks from the emission signal which helped identify the position of each configuration. Deconvolution of RXES data was accomplished via a non-linear least square fitting python module (LMFIT) [31], by using two skewed Lorentzian functions corresponding to the f^3 and f^2 peaks, and a third skewed Lorentzian function corresponding to the fluorescence peak (FP) when E_i approached E_T of 17.170 keV to account for the electrons excited to the continuum.

An example multiconfiguration peak deconvolution at 2.4 GPa is shown in Figure 7(a) where green and red peaks correspond to the $5f^3$ and $5f^2$ configurations, respectively, and the purple dashed FP corresponds to the non-resonant emission at selected E_i at 2.4 GPa. The areas under the curves are integrated, to calculate the respective peak coefficients, shown in Figure 7(b). The resulting normalized peak coefficient data were then fitted to an associated Lorentzian (for $5f^3$ and $5f^2$ peaks) and integrated to calculate the configuration weight at each pressure. A more detailed summary for peak deconvolution and error analysis is discussed in Supplementary Materials [13].

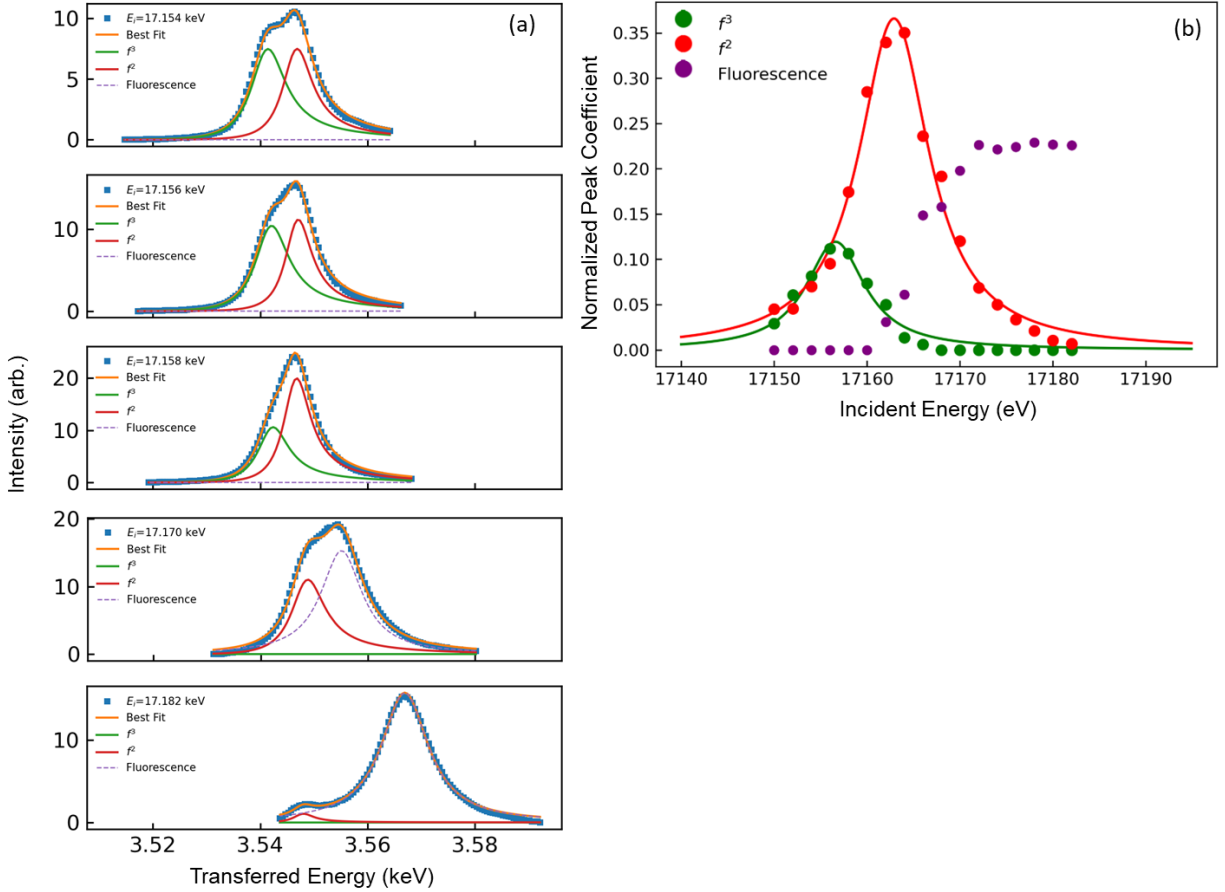


Figure 7. (a) Multiconfiguration peak deconvolution for $L_{\alpha 1}$ RXES at 2.4 GPa where green and red peaks correspond to the $5f^3$ and $5f^2$ peaks, respectively, and the purple dashed FP corresponds to the non-resonant emission. The FP dominates over $5f^3$ and $5f^2$ peaks when $E_i \geq 17170$ eV. (b) Normalized peak coefficient data plotted vs E_i . The fitted Lorentzians were integrated to calculate the configuration weights.

The $5f$ occupation (n_f) and f^3 and f^2 configuration fractions results are shown in Figure 8. At low-pressure, an initial $5f$ occupancy $n_f = \sim 2.26$ (valence of 3.74) at 1.8 GPa decreases with pressure until a minimum at ~ 2.8 GPa where $n_f \sim 2.21$ (valence of 3.79). Afterwards, n_f increases with pressure until ~ 15 GPa where a plateau appears at $n_f \sim 2.24$ (valence of 3.76) and persists up to 52 GPa, indicating that the $U\text{Te}_2$ valence stays mostly constant at high pressures. The nonmonotonic valence change preceding the pressure-induced phase transition (5 GPa) qualitatively agrees with Ref. [11] which claims a valence maximum at about 2 GPa. The movement of the valence towards $3+$ seems to be associated with the phase transition to the tetragonal structure which has more room for U atoms due to the larger d_{U-U} (see Figure 3). The increased volume can more easily accommodate the U^{3+} ion, which has a larger ionic radius than the U^{4+} ion. Stability of the valence above 15 GPa appears to be consistent with PFY-XAS data which exhibit little energy shift in the white-line position with pressure (see Figure 5). Although the PFY-XAS white-line shift can be due to both the change in n_f and in the localization of $5f$ -electrons [32], we do see some similarities between the PFY-XAS and RXES data, as manifested in the mirrored curves in Figures 5 and 8. The discrepancy between the two curves reflects the extra contribution to the PFY-XAS spectra from the change in the degree of itinerancy of $5f$ -electrons under pressure.

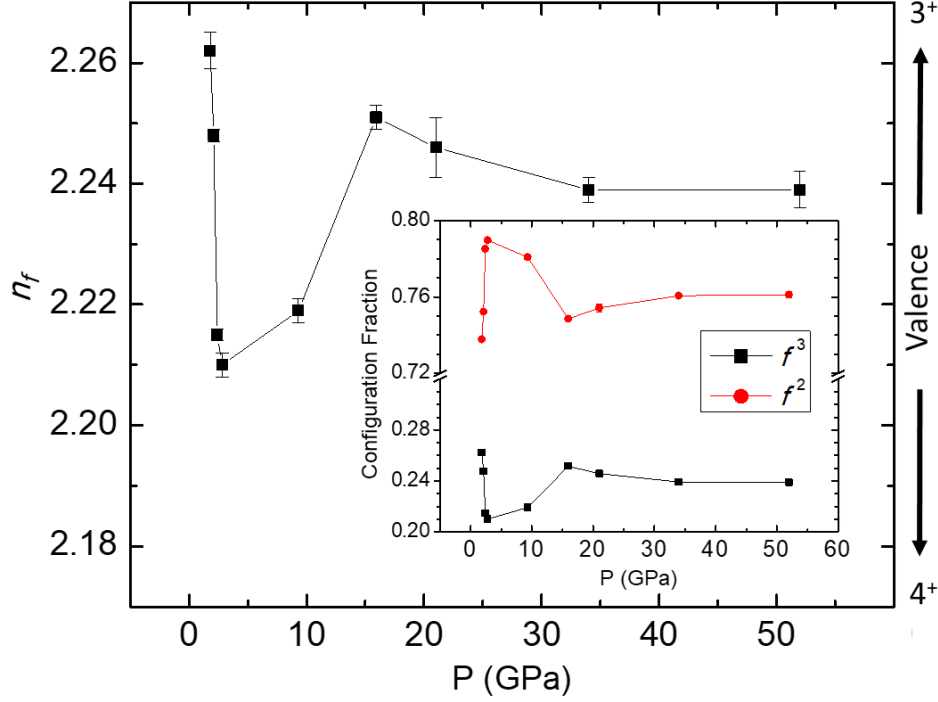


Figure 8. The calculated $5f$ occupation n_f , and configuration fractions of f^3 and f^2 (inset) as a function of pressure for UTe_2 at RT. The vertical bars indicate the estimated standard deviation (refer to Supplementary Materials [13]).

In a Kondo lattice, magnetic ordering of the lanthanide or actinide magnetic moments is mediated by conduction electrons whose spins interact with the lanthanide or actinide magnetic moments via the Ruderman-Kittel-Kasuya-Yosida RKKY interaction that varies to second order in the intra-atomic exchange interaction parameter $J_{ex} = -V_H^2/|\epsilon_f|$, where V_H represents the strength of hybridization between the localized f - and conduction electron-states and ϵ_f is the energy separating the localized f -electron state and the Fermi level E_F . In UTe_2 , with decreasing pressure in the lower pressure region (1.8 – 2.8 GPa), the valence changes towards 3+, coincident with the rapid suppression of the Néel temperature of the AFM phase [10, 33], followed by the appearance of two unconventional superconducting phases near ambient pressure and a corresponding heavy fermion normal state, reflected in the T -dependence of the electrical resistivity. This reveals the location of an AFM QCP in the UTe_2 Doniach phase diagram associated with the complete Kondo screening of the U magnetic moments induced by decreasing pressure. It would be interesting to determine if this is accompanied by a simultaneous valence change in the same pressure region. Additionally, it implies $|J_{ex}|$ increases with decreasing pressure, which is unusual because we expect $|J_{ex}|$ to decrease with decreasing pressure due to a decrease in V_H with decreasing pressure. Similarly, it infers $|\epsilon_f|$ decreases with decreasing pressure at a higher rate than that of V_H . This is similar to the scenario suggested for the relationship between the hidden order phase and the antiferromagnetic phase in the heavy fermion compound URu_2Si_2 [34]. In that case, pressure or chemical pressure via substitution of the smaller Fe atom for Ru drives the transition in URu_2Si_2 from the nonmagnetic hidden order phase, which exhibits coexisting unconventional superconductivity, to the AFM phase in the Doniach phase diagram due to a decrease in $|J_{ex}|$ with pressure [34].

Concluding Remarks

We studied the electronic and structural properties of UTe_2 via RXES up to 52 GPa and XRD up to 30 GPa, to higher pressures than previously [10, 11], and mapped the valence across the pressure induced structural phase transition between 5 and 7 GPa from $Immm$ (orthorhombic) to $I4/mmm$ (body centered tetragonal). Due to the higher energy resolution of the RXES technique compared to traditional XANES, we were able to calculate the change of the U valence with pressure. Observations indicate that UTe_2 as an f -electron system changes from a lower to a higher symmetry crystal structure under high pressure. This indicates that in the high-pressure tetragonal phase, $5f$ -electrons become more localized and less itinerant as one would expect from the viewpoint of a pressure induced increase in d_{U-U} . The d_{U-U} over the whole investigated pressure range (1.8 to 30 GPa) is larger than the Hill limit for U compounds, so magnetic ordering due to RKKY interactions could be anticipated. In reality, in this regime correlated electron phenomena such as unconventional superconductivity and heavy fermion behavior emerge. This implies that hybridization (V_H) between localized $5f$ - and conduction electron-states and on-site Coulomb repulsion (U) between $5f$ -electrons should play an important role in determining the electronic and magnetic properties of UTe_2 [8], like it does in other heavy fermion systems, contributing to the failure of using the Hill limit to categorize the degree of $5f$ itinerancy in UTe_2 .

At RT, RXES data show UTe_2 has a valence of ~ 3.74 at 1.8 GPa which changes to 3.79 at 2.8 GPa and then back to a value slightly smaller than that at 1.8 GPa. Interestingly, the change in valence is accompanied by the structural phase transition at 5 - 7 GPa, suggesting a correlation between the U valence and crystal structure of UTe_2 . At pressures higher than 15 GPa, the U valence does not change with pressure. PFY-XAS data also revealed a nonmonotonic change in the white-line position with pressure; however, due to complications associated with different mechanisms that lead to the shift in white-line position, it is difficult to reach a more definitive conclusion. It is worthwhile to point out that our PFY-XAS and RXES measurements were done at RT whereas other results regarding the UTe_2 valence were based on spectroscopic measurements at low temperature in Ref. [27] (20 K), Ref. [10] (1.7 K), and Ref. [11] (2.7 K). It is known that for $4f$ systems with a small Kondo temperature, n_f depends strongly on temperature (e.g., YbAgCu_4 , see [35]). Our RXES results demonstrate well-separated resonant emissions from $5f^3$ and $5f^2$ configurations, which illustrate the advantage of using RXES in determining UTe_2 valence. Extending RXES measurements to lower temperature, especially near the superconducting or magnetic ordering temperatures at high pressures, would reveal whether the U valence changes when UTe_2 undergoes these electronic and magnetic transitions.

Acknowledgments

Research at University of California, San Diego was supported by the National Nuclear Security Administration (NNSA) under the Stewardship Science Academic Alliance Program through the US DOE under Grant DE-NA0004086, and the US Department of Energy (DOE) Basic Energy Sciences under Grant DE-FG02-04ER46105. This work was sponsored in part by the UC San Diego Materials Research Science and Engineering Center (UCSD MRSEC), supported by the National Science Foundation (NSF) under Grant DMR-2011924. Research at the University of Illinois Chicago was supported by the NNSA (DE-NA-0003975, CDAC) and NSF (DMR-2119308). Research at Florida State University and the National High Magnetic Field Laboratory was supported by NSF Cooperative Agreement DMR-2128556, and the DOE. Portions of this work were performed at HPCAT (Sector 16), Advanced Photon Source (APS), Argonne National Laboratory. HPCAT operations are supported by DOE-NNSA's Office of Experimental Sciences. The Advanced Photon Source is a U.S. Department of Energy (DOE) Office of Science User Facility operated for the DOE Office of Science by Argonne National Laboratory under Contract No. DE-AC02-06CH11357. It is a pleasure to acknowledge informative discussions with Professor Andrea Severing, Professor Liu Hao Tjeng, Andrea Marino, and Denise Christovam. We thank Curtis Kenney-Benson for assistance with x-ray measurements at HPCAT.

References

- [1] Sheng Ran, Chris Eckberg, Qing-Ping Ding, Yuji Furukawa, Tristin Metz, Shanta R. Saha, I-Lin Liu, Mark Zic, Hyunsoo Kim, Johnpierre Paglione, and Nicholas P. Butch, “Nearly ferromagnetic spin-triplet superconductivity,” *Science* **365**, 684 (2019).
- [2] Dai Aoki, Ai Nakamura, Fuminori Honda, DeXin Li, Yoshiya Homma, Yusei Shimizu, Yoshiki J. Sato, Georg Knebel, Jean-Pascal Brison, Alexandre Pourret, Daniel Braithwaite, Gerard Lapertot, Qun Niu, Michal Vališka, Hisatomo Harima, and Jacques Flouquet, “Unconventional superconductivity in heavy fermion UTe_2 ,” *J. Phys. Soc. Jpn.* **88**, 043702 (2019).
- [3] Sheng Ran, I-Lin Liu, Yun Suk Eo, Daniel J. Campbell, Paul M. Neves, Wesley T. Fuhrman, Shanta R. Saha, Christopher Eckberg, Hyunsoo Kim, David Graf, Fedor Balakirev, John Singleton, Johnpierre Paglione and Nicholas P. Butch, “Extreme magnetic field-boosted superconductivity,” *Nat. Phys.* **15**, 1250 (2019).
- [4] Georg Knebel, William Knafo, Alexandre Pourret, Qun Niu, Michal Vališka, Daniel Braithwaite, Gérard Lapertot, Marc Nardone, Abdelaziz Zitouni, Sanu Mishra, Ilya Sheikin, Gabriel Seyfarth, Jean-Pascal Brison, Dai Aoki, and Jacques Flouquet, “Field-reentrant superconductivity close to a metamagnetic transition in the heavy-fermion superconductor UTe_2 ,” *J. Phys. Soc. Jpn.* **88**, 063707 (2019).
- [5] Y. Xiao, P. Chow, and G. Shen, “High pressure X-ray emission spectroscopy at the advanced photon source,” *High Press. Res.* **36**, 315-331 (2016).
- [6] C. H. Booth, Yu Jiang, D. L. Wang, J. N. Mitchell, P. H. Tobash, E. D. Bauer, M. A. Wall, P. G. Allen, D. Sokaras, D. Nordlund, T. -C. Weng, M. A. Torrez, and J. L. Sarrao, “Multiconfigurational nature of $5f$ orbitals in uranium and plutonium intermetallics,” *Proc. Natl. Acad. Sci. U.S.A.* **109**, 10205-10209 (2012).
- [7] F. Nasreen, D. Antonio, D. VanGennep, C. H. Booth, K. Kothapalli, E. D. Bauer, J. L. Sarrao, B. Lavina, V. Iota-Herbei, S. Sinogeikin, and P. Chow, “High pressure effects on $U L_3$ x-ray absorption in partial fluorescence yield mode and single crystal x-ray diffraction in the heavy fermion compound UCd_{11} ,” *J. Phys.: Condens. Matter* **28**, 105601 (2016).
- [8] Larissa Q. Huston, Dmitry Y. Popov, Ashley Weiland, Mitchell M. Bordelon, Priscila F. S. Rosa, Richard L. Rowland, II, Brian L. Scott, Guoyin Shen, Changyong Park, Eric K. Moss, S. M. Thomas, J. D. Thompson, Blake T. Sturtevant, and Eric D. Bauer, “Metastable phase of UTe_2 formed under high pressure above 5 GPa,” *Phys. Rev. Mat.* **6**, 114801 (2022).
- [9] Fuminori Honda, Shintaro Kobayashi, Naomi Kawamura, Saori Kawaguchi, Takatsugu Koizumi, Yoshiki J. Sato, Yoshiya Homma, Naoki Ishimatsu, Jun Gouchi, Yoshiya Uwatoko, Hisatomo Harima, Jacques Flouquet, and Dai Aoki, “Pressure-induced structural transition and new superconducting phase in UTe_2 ,” *J. Phys. Soc. Jpn.* **92**, 044702 (2023).
- [10] S. M. Thomas, F. B. Santos, M. H. Christensen, T. Asaba, F. Ronning, J. D. Thompson, E. D. Bauer, R. M. Fernandes, G. Fabbris, and P. F. S. Rosa, “Evidence for a pressure-induced antiferromagnetic quantum critical point in intermediate-valence UTe_2 ,” *Science Advances* **6**, eabc8709 (2020).
- [11] Wilhelm, F., Sanchez, J.P., Braithwaite, D., Knebel, G., Lapertot, G. and Rogalev, A., “Investigating the electronic states of UTe_2 using X-ray spectroscopy,” *Commun. Phys.* **6**, 1-7 (2023).
- [12] Chunruo Duan, R. E. Baumbach, Andrey Podlesnyak, Yuhang Deng, Camilla Moir, Alexander J. Breindel, M. Brian Maple, E. M. Nica, Qimiao Si, and Pengcheng Dai, “Resonance from antiferromagnetic spin fluctuations for superconductivity in UTe_2 ,” *Nature* **600**, 636 (2021).
- [13] Supplementary Information

- [14] D. R. Boehme, M. C. Nichols, R. L. Snyder, and D. P. Matheis, “An investigation of the tellurium-rich uranium tellurides using X-ray powder diffraction,” *J. Alloys Compd.* **179**, 37 (1992).
- [15] K. Hu, Y. Zhao, Y. Geng, J. Yu, and Y. Gu, “Pressure induced phase transition in heavy fermion metal UTe_2 : A first-principles study,” *Phys. Lett. A* **451**, 128401 (2022).
- [16] B. H. Toby and R. B. Von Dreele, “GSAS-II: the genesis of a modern open-source all purpose crystallography software package,” *J. Appl. Crystallogr.* **46**, 544-549 (2013).
- [17] K. Aoki, O. Shimomura, and S. Minomura, “Crystal structure of the high-pressure phase of tellurium,” *J. Phys. Soc. Jpn.* **48**, 551-556 (1980).
- [18] Y. K. Vohra and J. Akella, “ $5f$ bonding in thorium metal at extreme compressions: Phase transitions to 300 GPa,” *Phys. Rev. Lett.* **67**, 3563 (1991).
- [19] K. T. Moore and van der L. Gerrit, “Nature of the $5f$ states in actinide metals,” *Rev. Mod. Phys.* **81**, 235 (2009).
- [20] H. H. Hill, in “Plutonium 1970 and Other Actinides,” edited by W. N. Miner, the Metallurgical Society of the AIME, New York (1970).
- [21] N. Shekar, V. Kathirvel, B. Shukla, and P. Sahu, “Phase Transitions and Structural Stability of Binary Uranium Intermetallics Under High Pressure: A Review,” *Proc. Natl. Acad. Sci., India, Sect. A* **82**, 163 (2012).
- [22] N. W. Ashcroft and N. D. Mermin, *Solid State Physics*, (Saunders College, Philadelphia, 1976) 19, 374-379.
- [23] S. Liu, Y. Xu, E. C. Kotta, L. Miao, S. Ran, J. Paglione, N. P. Butch, J. D. Denlinger, Y. -D. Chuang, and L. A. Wray, “Identifying f -electron symmetries of UTe_2 with O-edge resonant inelastic x-ray scattering,” *Phys. Rev. B* **106**, L241111 (2022).
- [24] T. Vitova, K. O. Kvashnina, G. Nocton, G. Sukharina, M. A. Denecke, S. M. Butorin, M. Mazzanti, R. Caciuffo, A. Soldatov, T. Behrends, and H. Geckeis, “High Energy Resolution X-Ray Absorption Spectroscopy Study of Uranium in Varying Valence States,” *Phys. Rev. B* **82**, 2 (2010).
- [25] C. H. Booth, S. A. Medling, J. G. Tobin, R. E. Baumbach, E. D. Bauer, D. Sokaras, D. Nordlund, and T. C. Weng, “Probing $5f$ -State Configurations in URu_2Si_2 with U LIII -Edge Resonant X-Ray Emission Spectroscopy,” *Phys. Rev. B* **94**, 1 (2016).
- [26] M. Newville, “Larch: An Analysis Package for XAFS and Related Spectroscopies,” *Journal of Physics: Conference Series* **430**, 012007 (2013).
- [27] S. I. Fujimori, I. Kawasaki, Y. Takeda, H. Yamagami, A. Nakamura, Y. Homma, and D. Aoki, “Core-level photoelectron spectroscopy study of UTe_2 ,” *J. Phys. Soc. Jpn.* **90**, 015002 (2021).
- [28] A. F. Starace, “Potential-barrier effects in photoabsorption. I. General theory,” *Phys. Rev. B* **5**, 1773 (1972).
- [29] R. S. Kumar, A. Svane, G. Vaitheeswaran, V. Kanchana, E. D. Bauer, M. Hu, M. F. Nicol, and A. L. Cornelius, “Pressure-Induced Valence Change in $YbAl_3$: A Combined High-Pressure Inelastic X-Ray Scattering and Theoretical Investigation,” *Phys. Rev. B* **78**, 1 (2008).
- [30] J. P. Rueff, S. Raymond, A. Yaresko, D. Braithwaite, P. Leininger, G. Vankó, A. Huxley, J. Rebizant, and N. Sato, “Pressure-Induced f -Electron Delocalization in the U-Based Strongly Correlated Compounds UPd_3 and UPd_2Al_3 : Resonant Inelastic X-Ray Scattering and First-Principles Calculations,” *Phys. Rev. B* **76**, 1 (2007).
- [31] M. Newville, T. Stensitzki, D. B. Allen, and A. Ingargiola, “LMFIT: Non-Linear Least-Square Minimization and Curve-Fitting for Python,” Zenodo, 10.5281/zenodo.11813 (2014).

- [32] C. H. Booth, S. A. Medling, Yu Jiang, E. D. Bauer, P. H. Tobash, J. N. Mitchell, D. K. Veirs, M. A. Wall, P. G. Allen, J. J. Kas, D. Sokaras, D. Nordlund, and T. -C. Weng, "Delocalization and occupancy effects of 5f orbitals in plutonium intermetallics using L₃-edge resonant x-ray emission spectroscopy," *J. Electron Spectrosc. Relat. Phenom.* **194**, 57-65 (2014).
- [33] W. Knafo, T. Thebault, P. Manuel, D. D. Khalyavin, F. Orlandi, E. Ressouche, K. Beauvois, G. Lapertot, K. Kaneko, D. Aoki, D. Braithwaite, G. Knebel, and S. Raymond, "Incommensurate antiferromagnetism in UTe₂ under pressure," arXiv preprint arXiv:2311.05455 (2023).
- [34] A. Marino, D. S. Christovam, C. F. Chang, J. Falke, C. Y. Kuo, C. N. Wu, M. Sundermann, A. Amorese, H. Gretarsson, E. Lee-Wong, C. M. Moir, Y. Deng, M. B. Maple, P. Thalmeier, L. H. Tjeng, and A. Severing, "Fe substitution in URu₂Si₂: Singlet magnetism in an extended Doniach phase diagram," *Phys. Rev. B* **108**, 085128 (2023).
- [35] C. Dallera, E. Annese, J. P. Rueff, A. Palenzona, G. Vankó, L. Braicovich, A. Shukla, and M. Gioni, "Determination of Pressure-Induced Valence Changes in YbAl₂ by Resonant Inelastic X-Ray Emission," *Phys. Rev. B* **68**, 1 (2003).